Yu *et al.*
Chinese Journal of Mechanical Engineering (2022) 35:50
https://doi.org/10.1186/s10033-022-00721-4

Chinese Journal of Mechanical Engineering

ORIGINAL ARTICLE

Open Access

An Experimental Validation Study on Ferrofluid Evaporation

Wenjuan Yu[1], Decai Li[1,2*] and Sifang Niu[1]

Abstract

The current research on the evaporation of ferrofluids mainly focuses on the characterization of ultra-low vapor pressure ferrofluids in vacuum and the theoretical analysis of the evaporation process. Few studies have focused on the experimental validation of the proposed evaporation rate equations and on the comparison of the differences in ferrofluid evaporation. In this study, based on the Bolotov's model, an evaporation rate equation is deduced from the experimental model. The experimental study included a comparison of the evaporation, magnetic particle volume fraction, temperature, height of the fluid surface from the outlet, and magnetic field of a kerosene-based ferrofluid and its base carrier liquid. The prepared sample was evaporated in a test tube, and the evaporation rate was calculated by measuring the weight loss of the sample. The experimental results show that the evaporation rate of the base carrier liquid is higher than that of the ferrofluid. The smaller the volume fraction of the magnetic particles, the greater the evaporation rate. The magnetic particles play a key role in preventing evaporation of the base liquid. The higher the temperature, the smaller the deviation of the evaporation rate from the predicted value. The evaporation rates obtained by the two control groups at the height of the fluid surface from the outlet were lower than the predict value. The magnetic field had a certain promotional effect on the evaporation of the ferrofluid. The experimental results were consistent with the results obtained using Bolotov's model. This research validates Bolotov's model and shows that the model is somewhat biased but still responds well to different variables.

Keywords: Evaporation rate, Experimental study, Ferrofluid, Kerosene, Magnetic field, Validation

1 Introduction

A ferrofluid, also known as a magnetic fluid, is a nanoscale functional material, usually prepared via the co-precipitation method [1]. It is a colloidal suspension of single-domain magnetic particles, which is composed of three parts—the magnetic particles, surfactant, and base carrier liquid [2, 3]. The diameters of the magnetic particles range from 8 to 10 nm, and the particles are coated with surfactant to prevent agglomeration of the liquid and are dispersed in a base liquid. Ferrofluids have both the magnetic properties of a solid and the fluidity of a liquid. When no external magnetic field is applied, the ferrofluid acts as a Newtonian fluid. When a magnetic field is applied, the magnetic particles recombine, so that the entire ferrofluid becomes strongly magnetized and exhibits magnetism, showing non-Newtonian fluid behavior [4].

Since Stephen [5] first synthesized a ferrofluid in 1965, it has been applied in numerous industries including [6] dynamic sealing [7], heat conduction, damping [8], and drug targeting [9]. Magnetic fluid sealing is a new type of sealing method, which is different from the traditional sealing methods employed in the past. The magnetic fluid seal has the advantages of zero leakage, a long life, and high reliability [10–12]. For the practical application of magnetic fluid sealing devices, a magnetic fluid must exist in the gap between the pole tooth and the rotating shaft, forming several "O"-shaped sealing rings, which are responsible for the sealing effect [13–15]. However,

*Correspondence: lidecai@mail.tsinghua.edu.cn
[1] School of Mechanical Electronic and Control Engineering, Beijing Jiaotong University, Beijing 100044, China
Full list of author information is available at the end of the article

under the action of a magnetic field and a temperature field, the ferrofluid will evaporate, causing changes in the properties of the magnetic fluid and resulting in failure of the seal. To satisfy the high quality requirements and the harsh practical conditions—for example, for applications like monocrystalline silicon furnaces and optical devices—it is necessary to further study the evaporation of ferrofluids.

Numerous studies have focused on this aspect. Some researchers started with a focus on the preparation of new ferrofluids with low evaporation rates. For example, Bottenberg and Chagnon [16] prepared a polyphenylene ether-based ferrofluid. Compared with hydrocarbon-based ferrofluids, this ferrofluid has a lower saturated vapor pressure, which can reach 10^{-5} Pa at 20 °C. It is especially suitable for sealing under high vacuum environments. Black et al. [17] prepared and characterized a Perfluoropolyether (PFPE)-based ferrofluid and found that it showed low volatility at high temperatures. Li and Raj [18] calculated the evaporation rate of hydrocarbon-based and fluorocarbon-based ferrofluids under four different vacuum levels. It was found that under higher vacuum levels the evaporation rate of two ferrofluids were significantly higher than under atmospheric conditions, and the fluorocarbon-based magnetic fluids are more suitable for ultra-high-vacuum applications. The preparation of ferrofluids with low saturated vapor pressure, which is very important for the selection of the base carrier liquid and surfactant, is a challenging task under research settings. Although the evaporation rate of ferrofluids with low saturated vapor pressure has been significantly improved, the stability of ferrofluids remains unsatisfactory. Some researchers have used the evaporation of droplets to study the evaporation mechanism of ferrofluids. Cristaldo et al. [19, 20] numerically analyzed the heating process of a ferrofluid droplet under an alternating magnetic field with a thermal boundary layer model and showed that because of the alternating magnetic field, the interior of the thermal boundary could layer rapidly reach the boiling point, thereby increasing the droplet evaporation rate. Bolotov et al. [21, 22] derived equations of the evaporation rate to estimate the life of a tribounit with ferrofluid under a vacuum and gas atmosphere, but scarely any experiments were performed to verify it. Jaiswal et al. [23] and Chattopadhyay et al. [24] studied the evaporation kinetics of a magnetic salt solution pendant droplet under a horizontal magnetic field. Their experimental observations revealed that the evaporation rate was enhanced with a magnetic field, and magneto-solutal advection was thought to be the controlling factor for the augmented evaporation rate. Jadav et al. [25] placed water-based magnetic droplets on a flat glass substrate and studied the influence of a magnetic field on the evaporation rate and contact angle. The results showed that in the dry droplets, the structure and distribution of the nanomagnetic particles were related to the direction and magnitude of the applied field. Harikrishnan et al. [26] distinguished individual surfactants, particles, and the combined role of surfactants and particles in regulating evaporation kinetics, showing that the combined colloidal system of nanoparticles and surfactants exhibited the largest evaporation rate. This rate is a strong function of particle and surfactant concentration, revealing the role of surfactant in regulating the evaporation rate of colloidal solutions. Shyam et al. [27] studied the evaporation kinetics of a fixed ferromagnetic droplet placed on a soft substrate under the action of a time-dependent magnetic field. The time-varying magnetic field can effectively control the evaporation time of the ferromagnetic droplets; they also determined the critical frequency of the applied magnetic field strength, which makes the droplets encounter the minimum lifetime. At the critical frequency, the advection time scale of the magnetic nanoparticles is balanced by the magnetic disturbance time scale. Karapetsas

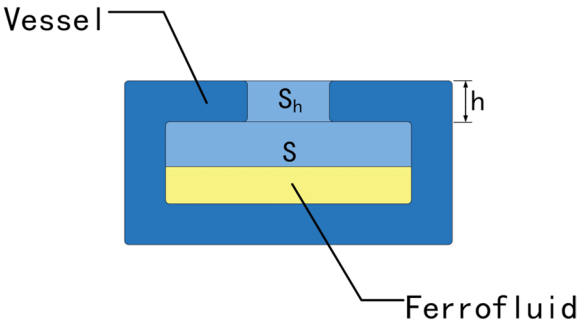

Figure 1 Ferrofluid in a vessel with a hole

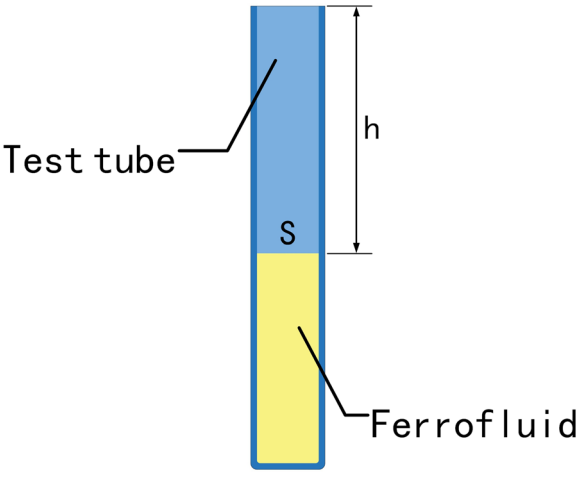

Figure 2 Ferrofluid in a test tube

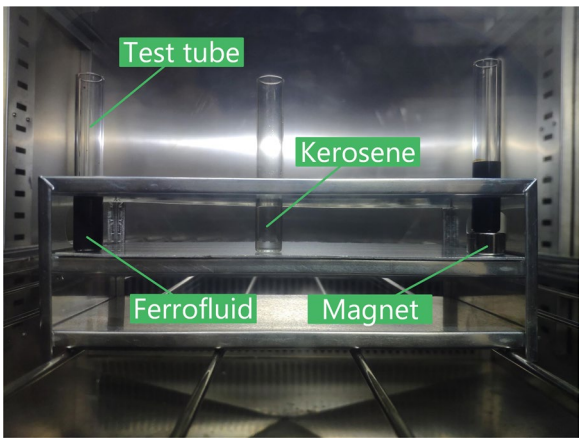

Figure 3 Sample in a high temperature test chamber

et al. [28] considered the flow dynamics of evaporating droplets in the presence of insoluble surfactants and a large number of non-interacting particles, and numerical calculations showed that the droplet lifetime was significantly affected by the balance between surfactant-enhancing diffusivity, inhibiting thermal Marangoni stress-induced motion and impeding the evaporative flux by reducing the effective interfacial area. Saroj and Panigrah [29] studied the evaporation of immobilized ferrofluid droplets on PDMS substrates and showed that the evaporation rate of the droplets increased with an increase in the ferrofluid concentration. In addition, they studied the "coffee-ring effect [30]" of the ferrofluid; it is believed that the magnetic field leads to a uniform deposition pattern of dry droplets.

Previous studies mainly focused on the characterization of an ultra-low vapor pressure ferrofluid in a vacuum and theoretical analysis of its evaporation process. However, there is a lack of studies on the verification of the proposed equations and the comparison of the differences between ferrofluid evaporation with and without a magnetic field in an experimental manner. In this study, we analyzed the evaporation rate of a kerosene-based ferrofluid under normal pressure with and without

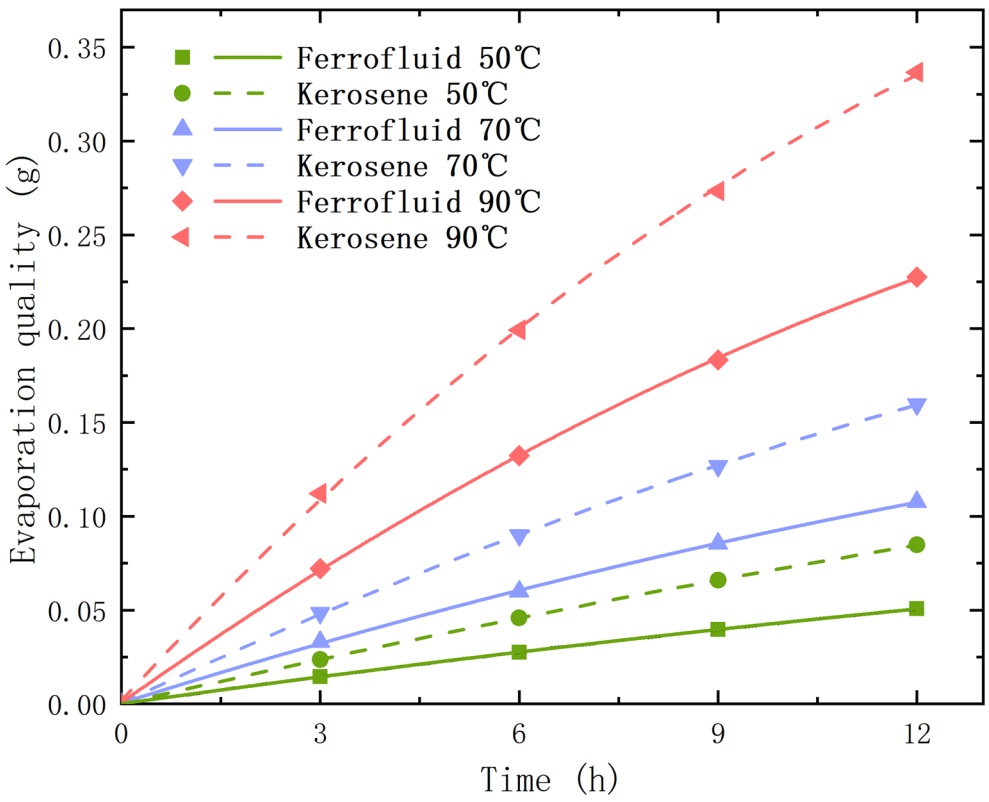

Figure 4 Weight loss of samples and their fitted curves at different temperatures

a magnetic field through experimental and theoretical studies.

2 Theoretical Research

Bolotov et al. [22] derived the evaporation rate equation of a ferrofluid from Fick's first law under several conditions. When the ferrofluid is in a vessel enclosed in a shell with a hole, as shown in Figure 1, the equation can be written as follows:

$$W = \frac{DS_h p_s \mu}{R_0 T h}(1-\omega_s)\left(1+\frac{DS_h}{\alpha h S(1-\omega_s)}\sqrt{\frac{2\pi\mu}{R_0 T}}\right)^{-1}, \tag{1}$$

where W is evaporation rate of the ferrofluid, g/s; D is diffusion coefficient of the vapor molecules, m^2/s; S_h is surface area of the hole, m^2; P_s is saturated vapor pressure of the base fluid, Pa; μ is molar mass of the base fluid, g/mol; R_0 is universal gas constant, J/(mol·K); T is absolute temperature of the ferrofluid, K; h is thickness of the hole, m; S is surface area of the ferrofluid, m^2; α is evaporation coefficient of the ferrofluid; ω_s is volume fraction of the magnetic particles.

According to Eq. (1), for the condition in which the ferrofluid is in a vessel like a test tube, as shown in Figure 2, $S = S_h$, where h is the height from the surface of ferrofluid to the mouth of test tube. The equation can be written as follows:

$$W = \frac{DSp_s\mu}{R_0 T h}(1-\omega_s)\left(1+\frac{D}{\alpha h(1-\omega_s)}\sqrt{\frac{2\pi\mu}{R_0 T}}\right)^{-1}. \tag{2}$$

To predict the evaporation rate using Eq. (2), the coefficients α and D must be determined. In certain cases, coefficient α can be less than 1, but for most substances, $\alpha \approx 1$ [21]. Coefficient D can be calculated in reverse from the evaporation rate of the base fluid under a certain temperature and atmospheric pressure. The following equation can be used to obtain the D under other conditions:

$$D = D_0 \frac{p_{A0}}{p_A}\left(\frac{T}{T_0}\right)^{3/2}, \tag{3}$$

where D_0 is the known diffusion coefficient at temperature T_0 and atmospheric pressure p_{A0}, and D is the unknown diffusion coefficient at temperature T and atmospheric pressure p_A.

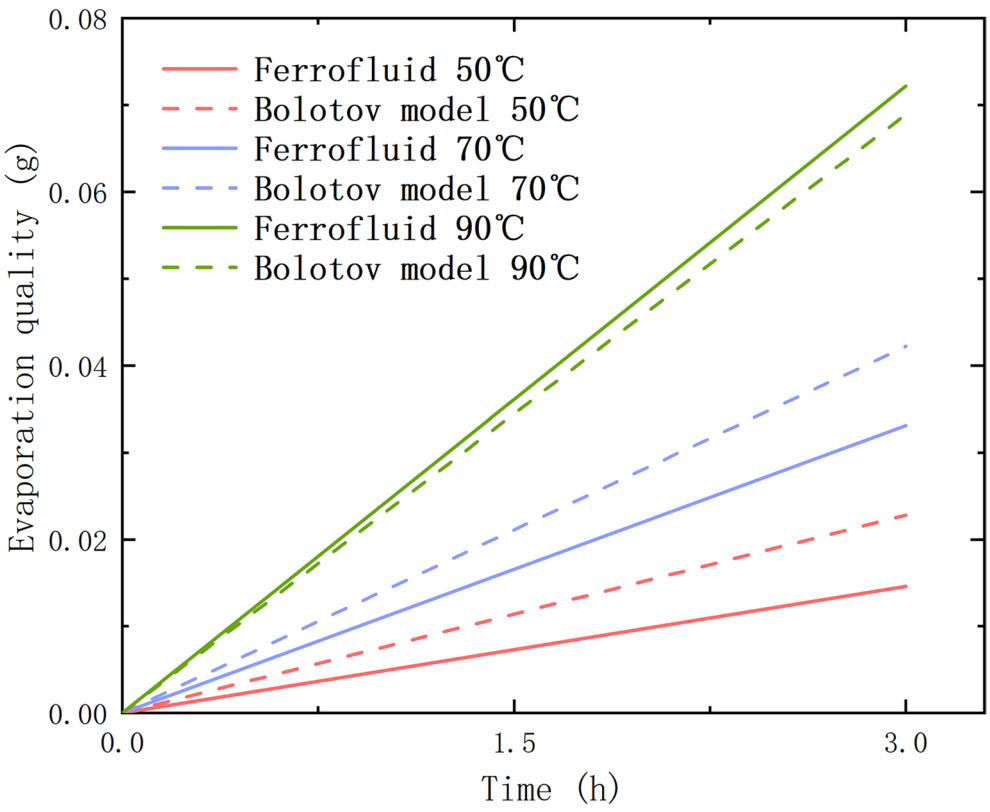

Figure 5 Prediction of the evaporation rate of a ferrofluid at different temperatures

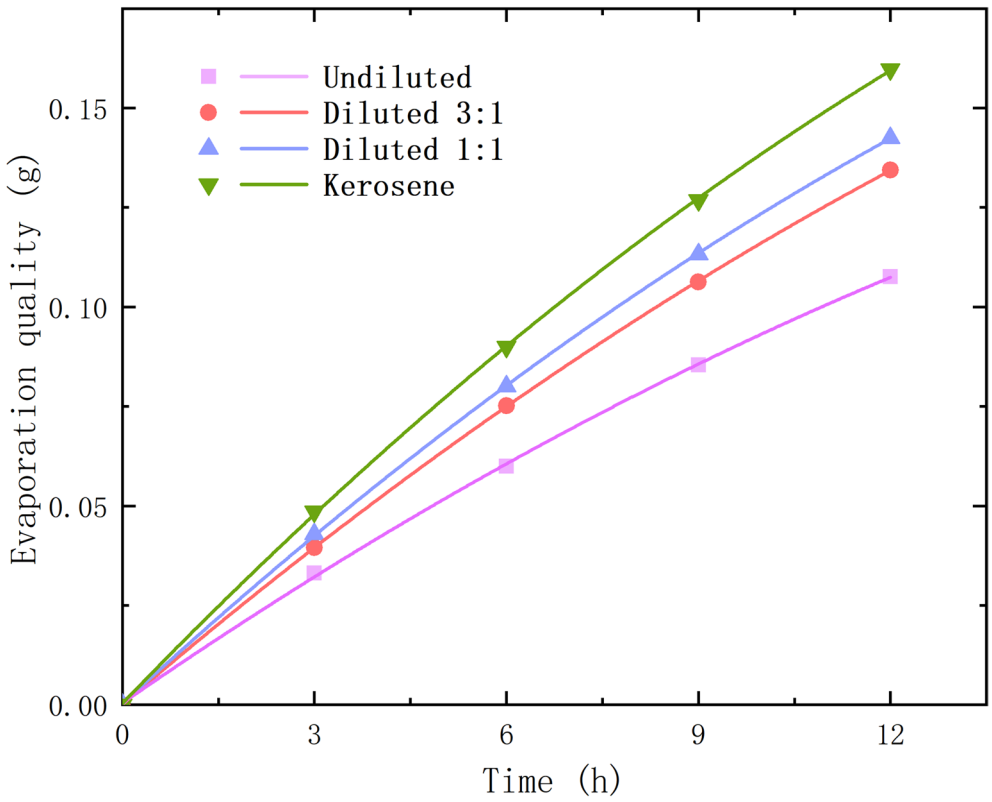

Figure 6 Weight loss of samples and their fitted curves with different dilution rates

3 Experimental Study

3.1 Experimental Materials and Devices

The materials used in the experiment were kerosene and kerosene-based ferrofluids with different volume fractions. The magnets used were N35 NdFeB cylindrical permanent magnets, which manufactured by Shanghai Siyuan Magnetic Industry, with a diameter of 16 mm, a thickness of 10 mm, a remanence B_r of 1.2 T, a coercive force H_c of 880 kA/m, and the maximum magnetic energy product (BH)max of 270 kJ/m^3.

The device used in the experiment was the Hefei Anke Environmental Testing Equipment, and a GDJS-1000L high and low temperature alternating damp heat test box with a temperature range of − 70 ℃ to + 150 ℃, and a temperature error of ± 0.5 ℃. A cylindrical flat-bottomed transparent borosilicate glass test tube with a total height of 76 mm and an inner diameter of 10 mm was used. An ME55 balance (METTLER TOLEDO), with a division value of 0.01 mg was also used.

3.2 Experimental Method

To verify the evaporation rate of the ferrofluid using Eq. (2), a kerosene-based ferrofluid and its base fluid kerosene were tested. A test tube, with a height and inner diameter of 76 mm and 10 mm, respectively, was filled with the sample. In some cases, a magnet was placed under the test tube to form a magnetic field. The test tube was placed in a high temperature test chamber for 12 h, as shown in Figure 3. During the process of evaporation, the sample's weight was measured every 3 h using a precision electronic balance with a resolution of 0.01 mg to obtain the weight loss data. The height h was controlled to ensure that the influence of the magnetic field on the surface area S was as small as possible.

The volume fraction ω_s was obtained from the density of sample and was ~ 13%. To prepare ferrofluids with different volume fractions, the samples were diluted with the base fluid and then were subjected to ultrasonic

treatment for an hour. Both the saturated vapor pressure p_s and molar mass μ were obtained from handbooks [31].

4 Results and Discussion

4.1 Temperature

To study the influence of temperature on the evaporation process, the ferrofluid and kerosene were placed in the chamber at 50 °C, 70 °C, and 90 °C with a height $h = 41$ mm and $\omega_s = 13\%$. Figure 4 presents the weight loss of the samples, which reveals that the evaporation rate of the ferrofluid is lower than that of its base fluid. However, it also shows that the curve of weight loss is nearly a straight line but not strictly a straight line, and the curve's gradient (evaporation rate) shows a reducing trend. According to Eq. (2), this phenomenon can be attributed to the increase of h and ω_s in the evaporation process. To make the calculating conditions more consistent with practical conditions, only the dataset of the first three hours was selected to represent the evaporation rate of the samples.

Before the calculation using Eq. (2) to predict the evaporation rate of the ferrofluid, the diffusion coefficient D was calculated in reverse using the evaporation rate of kerosene at 70 °C, which $D_0 = 1.9964 \times 10^{-6}$ m^2/s. The predicted evaporation rates of the ferrofluid at different temperatures are shown in Figure 5, which indicates that the deviation of the predicted values and the experimental values decreases with increasing temperature.

4.2 Volume Fraction

A ferrofluid with different volume fractions was prepared to study the relationship between the evaporation rate and the volume fraction when the sample evaporates with a height $h = 41$ mm at 70 °C. The ferrofluid was diluted with kerosene in a proportion of 3:1 and 1:1. Figure 6 presents the result of the experiment, which reveals that the evaporation rate of diluted ferrofluid shows an intermediate between those of the undiluted ferrofluid and kerosene. The more dilute the ferrofluid, the faster it evaporates, which clearly proves that the magnetic particles prevent the base fluid from evaporating. Figure 7 shows that the prediction values based on Eq. (2) are overestimated, but still reflect the difference between different dilution rates.

4.3 Height

Height h was also investigated as a variable. Undiluted samples with different heights, $h = 41$ mm and $h = 46$ mm, were tested at 70 °C. Figure 8 shows the result of the experiment which reveals that the higher the value

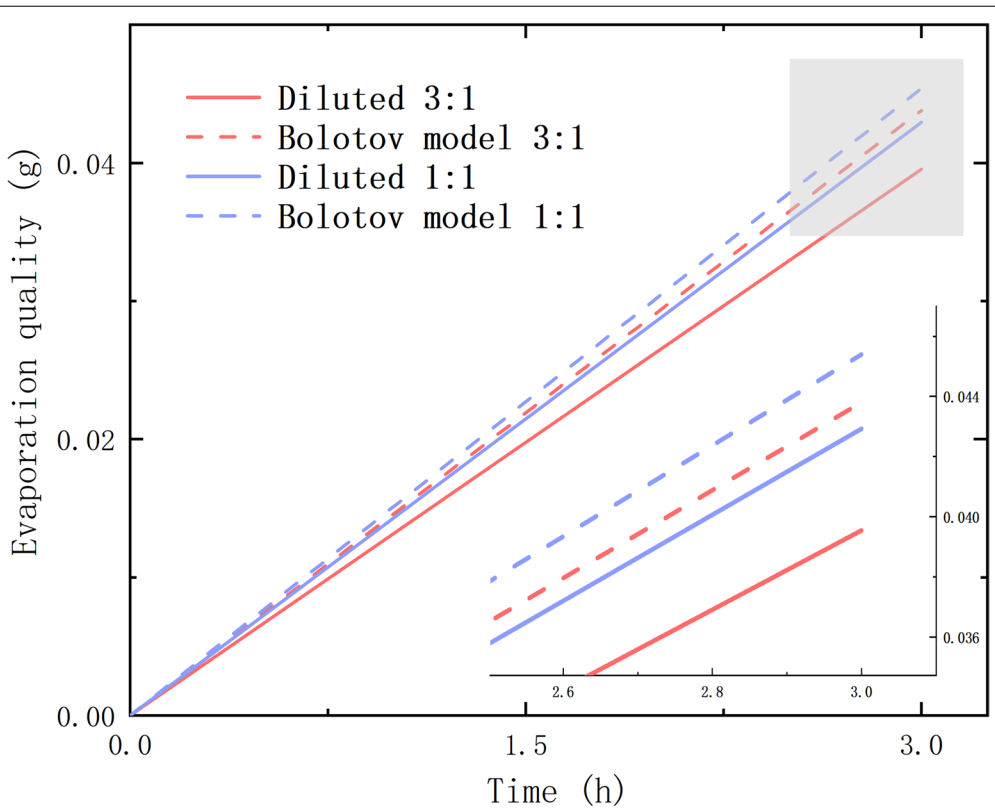

Figure 7 Prediction of the evaporation rate of the ferrofluid with different dilution rates

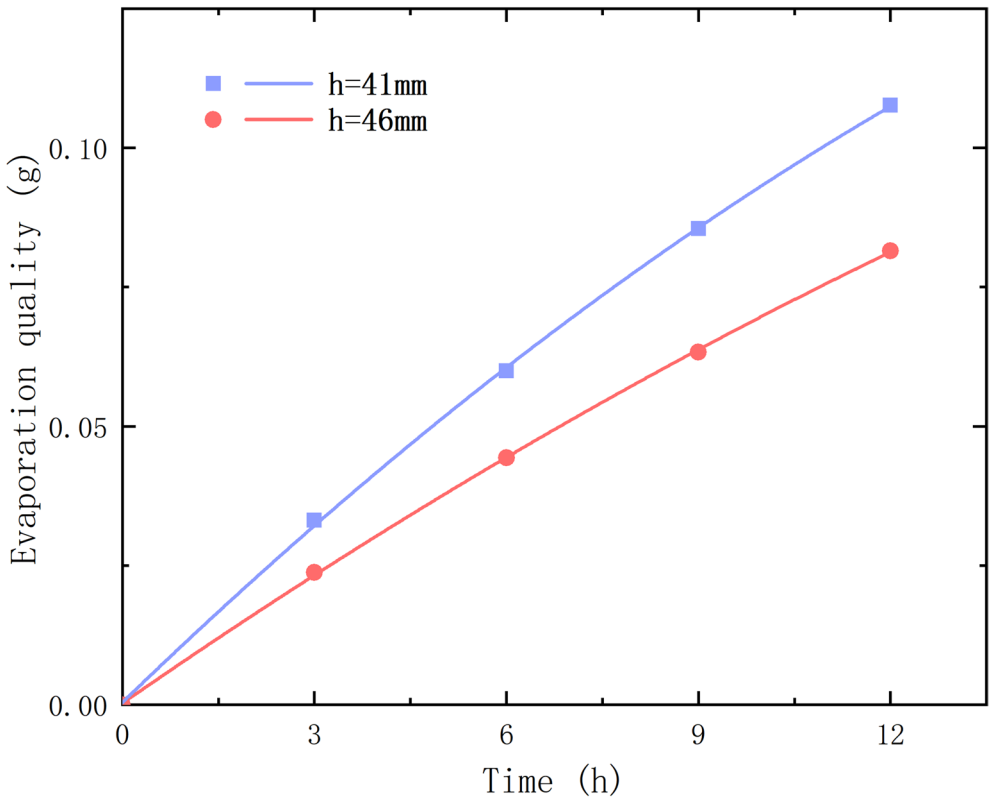

Figure 8 The weight loss of samples and their fitted curves with different height

of h, the slower the evaporation. Because the height changed in the case of $h = 46$ mm, the diffusion coefficient D had to be recalculated and was found to be $D_0 = 1.8941 \times 10^{-6}$ m^2/s. The predicted rates are given in Figure 9, which shows the same overestimated results as Sections 4.1 and 4.2.

4.4 Magnetic Field

The most distinguishing feature of a ferrofluid is the response of the magnetic particles dispersed in a base liquid to a magnetic field. Considering that the evaporation process of the base fluid is weakened by the magnetic particles, it is necessary to explore the influence of the magnetic field on the evaporation rate. An explorative experiment was designed to compare the cases with and without a magnetic field applied to the bottom of test tube. Undiluted samples were placed in the chamber with a height $h = 41$ mm at 70 °C.

Figure 10 shows that the evaporation of a ferrofluid to which a magnetic field is applied is intermediate between that of a ferrofluid to which a magnetic field is not applied and that of kerosene. This phenomenon might be attributed to the reduction in the local concentration near the ferrofluid surface, which makes the ferrofluid with a lower volume fraction evaporate.

5 Conclusions

We analyzed the evaporation rate of a kerosene-based ferrofluid with different variables using experimental studies and predicted the evaporation rate based on Bolotov's model. Our conclusions are listed as follows:

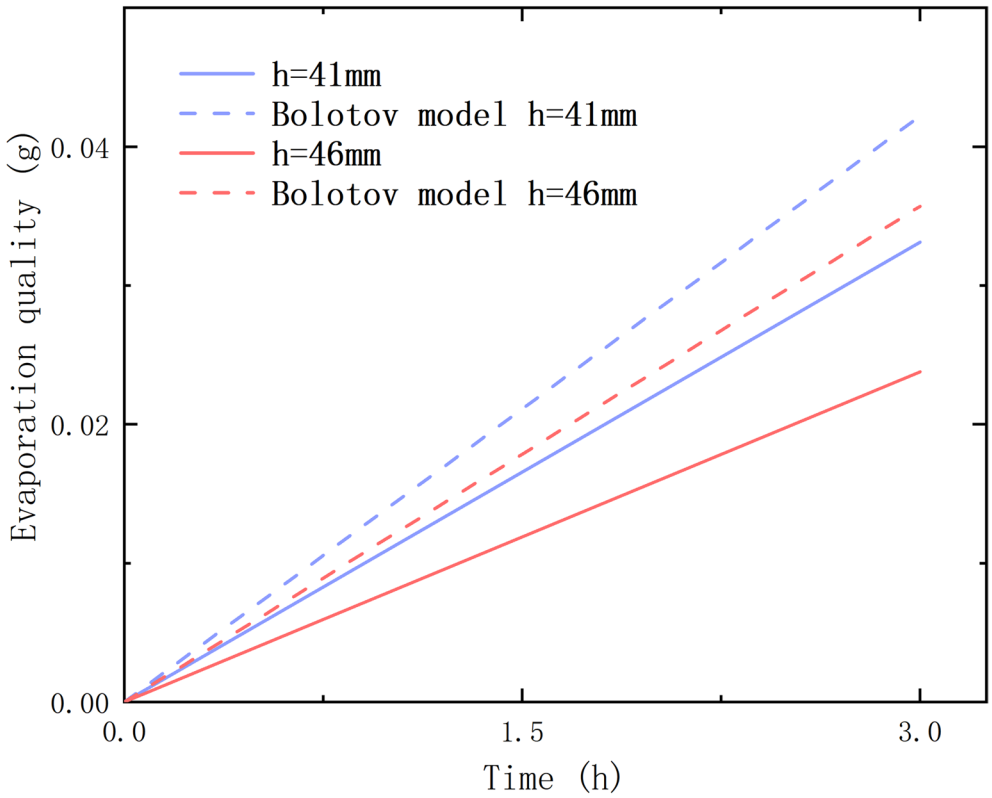

Figure 9 Prediction of the evaporation rate for ferrofluid with different heights

(1) Ferrofluids have a lower evaporation rate than the base fluid. The magnetic particles prevent the base fluid from evaporating, and a lower volume fraction leads to a higher evaporation rate.
(2) Although the results obtained using Bolotov's model show a certain deviation from the experimental results, the model still responds well to different variables.
(3) The magnetic field promotes the process of evaporation, which might be attributed to the reduction in the local concentration near the ferrofluid surface.

Because Bolotov's model is merely based on the loss of surface area S due to the magnetic particles covering the evaporation surface, it is reasonable to guess that there are other factors that affect the evaporation rate, which needs further study.

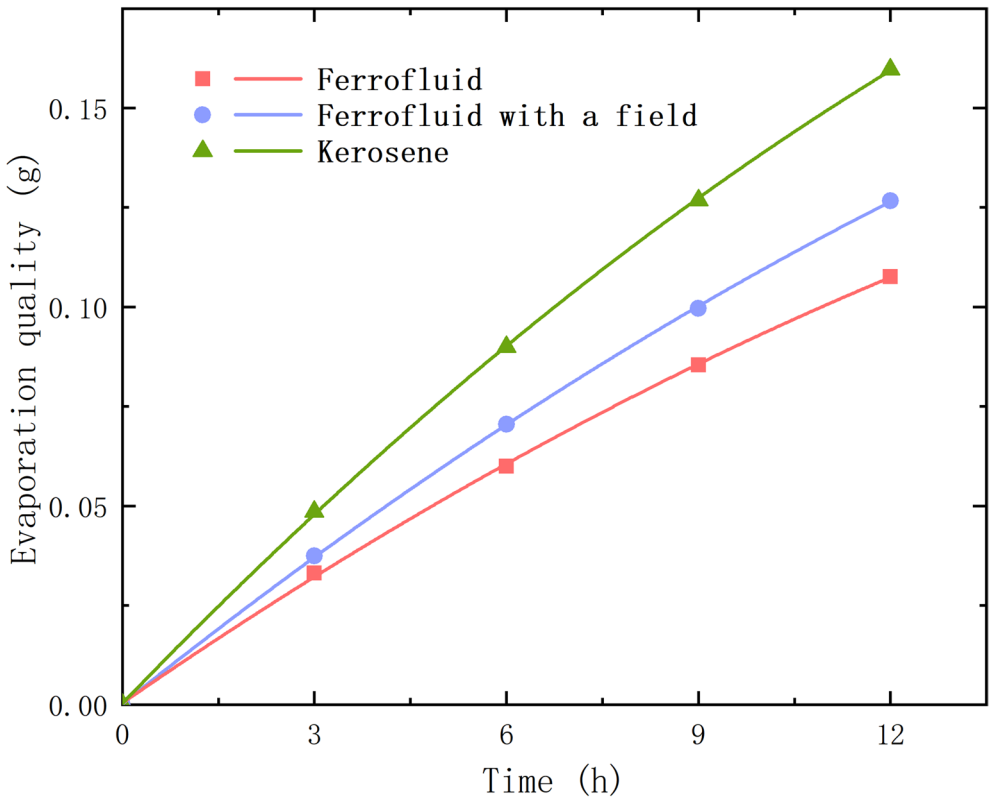

Figure 10 Weight loss of samples and their fitted curves with and without a magnetic field

Acknowledgements
Not applicable.

Author Contributions
DL was in charge of the whole trial; WY and SN wrote the manuscript and did laboratory analyses. All authors read and approved the final manuscript.

Authors' Information
Wenjuan Yu, born in 1996, is currently a PhD candidate at *School of Mechanical Electronic and Control Engineering, Beijing Jiaotong University, China*. Her research direction is the theory and application of ferrofluids.
Decai Li, born in 1965, is currently a tenured professor at *State Key Laboratory of Tribology, Tsinghua University, China*. His research direction is the theory and application of ferrofluids.
Sifang Niu, born in 1996, was graduated from *Beijing Jiaotong University, China*, in 2021 with a master's degree.

Funding
Supported by National Natural Science Foundation of China (Grant Nos. 51735006, 51927810, U1837206), and Beijing Municipal Natural Science Foundation of China (Grant No. 3182013).

Competing Interests
The authors declare no competing financial interests.

Author Details
[1]School of Mechanical Electronic and Control Engineering, Beijing Jiaotong University, Beijing 100044, China. [2]State Key Laboratory of Tribology, Tsinghua University, Beijing 100084, China.

Received: 7 July 2021 Revised: 19 March 2022 Accepted: 8 April 2022
Published online: 04 May 2022

References

[1] D C Li. *Theory and application of magnetic fluid seal*. Beijing: Science Press, 2010. (in chinese)
[2] X Liu, D C Li. Modeling the effect of surfactant (linoleic acid/oleic acid/stearic acid) on the stability of kerosene-based magnetic fluid with Fe_3O_4. *Functional Materials Letters*, 2021, 14(6): 1-12.
[3] S D Han, H C Cui, Z L Zhang, et al. Preparation method of magnetic fluid and introduction of several special magnetic fluid. *Functional Materials*, 2021, 52(10): 10061-10068.(in chinese)
[4] C Q Chi. *Physics basis and application of ferrofluid*. Beijing: Beihang University Press, 2011. (in chinese)
[5] P S Stephen. Low viscosity magnetic fluid obtained by the colloidal suspension of magnetic particles: US, 3215572A. 1965-11-02.
[6] D C Li. *Theory and application of magnetic fluid*. Beijing: Science Press, 2003. (in chinese)
[7] F Yuan, S Q Wang, D C Li, et al. Theoretical research on the novel magnetic fluid seal structure and its pressure resistance. *Journal of Mechanical Engineering*, 2022, 58(3): 213-220.(in chinese)
[8] J Yao, X Y Zhao, Z K Li, et al. Force optimization and damping performance of a novel ferrofluid inertial damper based on the levitation principle of ferrofluids. *Journal of Vibration Engineering & Technologies*, 2022: 1-13.
[9] A Gul, E Tzirtzilakis, S S Makhanov. Simulation of targeted magnetic drug delivery: Two-way coupled biomagnetic fluid dynamics approach. *Physics of Fluids*, 2022, 34(2): 1-14.

[10] Y J Zhang, Y B Chen, D C Li, et al. Experimental validation and numerical simulation of static pressure in multi-stage ferrofluid seals. *IEEE Transactions on Magnetics*, 2019, 55(3), 1-8.
[11] X L Yang, Y Guan, Y Y Huang. Numerical and experimental study of the embedded magnetic fluid seal with a small gap. *Physica Scripta*, 2021, 96(12): 1-14.
[12] X R Li, Z G Li, B S Zhu, et al. Optimal design of large gap magnetic fluid sealing device in a liquid environment. *Journal of Magnetism and Magnetic Materials*, 2021, 540: 1-11.
[13] W J Yu, D C Li, Y W Li, et al. Research on magnetic fluid seal of small vacuum coating machine. *Journal of Beijing Jiaotong University*, 45(5): 124–129 (in chinese).
[14] S F Niu. *Theoretical and experimental research on key issues of magne-tic fluid seal for electro-optical pod*. Beijing: Beijing Jiaotong Univer-sity, 2021 (in chinese).
[15] Y H Cheng, D C Li, Z K Li. Influence of rheological properties on the starting torque of magnetic fluid seal. *IEEE Transactions on Magnetics*, 2021, 57(3):1-8.
[16] W R Bottenberg, M S Chagnon. Low-vapor-pressure ferrofluids and method of making same: US, 4315827. 1982-2-16.
[17] T Black, K Raj, S Tsuda. Characterization of an ultra-low vapor pressure ferrofluid. *Journal of Magnetism and Magnetic Materials*, 2002, 252(1-3): 39-42.
[18] Z Li, K Raj. Effect of vacuum level on evaporation rate of magnetic fluids. *Journal of Magnetism and Magnetic Materials*, 2005, 289: 43-46.
[19] C F C Cristaldo, M M Vargas, F F Fachini. Ferrofluid droplet vaporiza-tion under very large magnetic power: Effects of pressure and effective thermal conductivity of liquid. *Proceedings of the Combustion Institute*, 2015, 35(2): 1613-1620.
[20] C F C Cristaldo, F F Fachini. Analysis of ferrofluid droplet combustion under very large magnetic power. *Combustion and Flame*, 2013, 160(8): 1458-1465.
[21] A Bolotov, V Novikov, O Novikova. Service life of magnetic liquid vacuum tribounits. *Procedia Engineering*, 2016, 150: 468-474.
[22] A Bolotov, V Novikov, O Novikova. Life of magnetic-fluid frictional components in gas. *Russian Engineering Research*, 2017, 37(1): 27-31.
[23] V Jaiswal, R K Dwivedi, A Harikrishnan, et al. Magnetohydrodynamics and magnetosolutal-transport-mediated evaporation dynamics in paramagnetic pendant droplets under field stimulus. *Physical Review E*, 2018, 98(1): 1-14.
[24] A Chattopadhyay, R K Dwivedi, A Harikrishnan, et al. Ferro-advection aided evaporation kinetics of ferrofluid droplets in magnetic field ambience. *Physics of Fluids*, 2020, 32(8): 1-12.
[25] M Jadav, R J Patel, R V Mehta. Influence of magnetic field on evaporation of a ferrofluid droplet. *Journal of Applied Physics*, 2017, 122(14): 1-8.
[26] A R Harikrishnan, P Dhar, S Gedupudi, et al. Oscillatory solutothermal convection-driven evaporation kinetics in colloidal nanoparticle surfactant complex fluid pendant droplets. *Physical Review Fluids*, 2018, 3(7): 1-21.
[27] S Shyam, P K Mondal, B Mehta. Field driven evaporation kinetics of a sessile ferrofluid droplet on a soft substrate. *Soft Matter*, 2020, 16(28): 6619-6632.
[28] G Karapetsas, K C Sahu, O K Matari. Evaporation of sessile droplets laden with particles and insoluble surfactants. *Langmuir*, 2016, 32(27): 6871-6881.
[29] S K Saroj, P K Panigrahi. Drying pattern and evaporation dynamics of sessile ferrofluid droplet on a PDMS substrate. *Colloids and Surfaces A: Physicochemical and Engineering Aspects*, 2019, 580: 1-13.
[30] P J Yunker, T Still, M A Lohr, et al. Suppression of the coffee-ring effect by shape-dependent capillary interactions. *Nature*, 2011, 476 (7360): 308–311.
[31] J R Zhang, T Y Zhao. *Handbook of thermophysical properties of materials commonly used in engineering*. Beijing: National Defense Industry Press, 1987. (in chinese)